

Nanoscale

Accepted Manuscript



This is an *Accepted Manuscript*, which has been through the Royal Society of Chemistry peer review process and has been accepted for publication.

Accepted Manuscripts are published online shortly after acceptance, before technical editing, formatting and proof reading. Using this free service, authors can make their results available to the community, in citable form, before we publish the edited article. We will replace this *Accepted Manuscript* with the edited and formatted *Advance Article* as soon as it is available.

You can find more information about *Accepted Manuscripts* in the [Information for Authors](#).

Please note that technical editing may introduce minor changes to the text and/or graphics, which may alter content. The journal's standard [Terms & Conditions](#) and the [Ethical guidelines](#) still apply. In no event shall the Royal Society of Chemistry be held responsible for any errors or omissions in this *Accepted Manuscript* or any consequences arising from the use of any information it contains.

ARTICLE

The Role of Nanoparticle Monolayer on the Flowing Behaviour of Polymer Melts in Nanochannels

Cite this: DOI: 10.1039/x0xx00000x

Received 00th January 2012,
Accepted 00th January 2012

DOI: 10.1039/x0xx00000x

www.rsc.org/

Long-Biao Huang,^{ab} Ye Zhou,^{ab} Su-Ting Han,^{ab} Yan Yan,^{ab} Li Zhou,^{ab} and V. A. L. Roy^{*ab}

Understanding and controlling the flowing of polymer melts at nanoscale is of great relevance for fundamental research and various applications. Here, we experimentally analyse the polymer flowing behaviour in a nanochannel of different roughness, fabricated by noble metal nanoparticle absorption. The experimental results show that nanochannel roughness significantly influences the surface energy eventually affecting the flowing behaviour of polymer melts. These results provide fundamental information on the preparation of one-dimensional polymer nanochannels applicable for micro/nano-injection technology.

Introduction

Understanding and controlling the flowing of liquids/melts at the nanoscale is of great relevance to fundamental research^{1, 2} and various applications such as micro/nanofluidic in medicine^{3, 4}, sensors⁵, solar cells^{6, 7}, lab-on-chip⁸. Comparing with simple liquid⁹⁻¹¹, however, the flowing behaviour of polymer melts in nanoscale such as nanochannel mainly stay on the simulation analysis¹²⁻¹⁶ due to the difficulty of obtaining polymer melts.

The flowing processes of liquid/melts are mainly affected by bulk properties of liquid/melts¹⁷⁻¹⁹, surface properties of nanochannels²⁰⁻²³ and others. By surface-modification of octadecyltrimethoxysilane, the flowing behaviour of polyethylene was significantly slowed down due to the reduction in surface energy²⁴. However, the other surface conditions such as roughness still need to be investigated.

On this regard, to investigate the influence of surface roughness of nanochannel on the flowing behaviour of polymer melts, nanoporous anodic alumina template (AAO) with well-ordered cylindrical pores has been employed to study the flowing behaviour of polymer melts²⁴⁻²⁶. Due to the surface-modification capability, thermal stability and mechanical rigidity of AAO, the cylindrical nanochannel with tunable diameters provides an ideal environment to investigate the flowing behaviour of polymer melts in nanoscale. In general, polymer melts are absorbed into nanochannels due to higher surface energy of AAO^{27, 28}. By measuring the displacement

length of polymer melts in AAO nanochannels, the flowing behaviour of polymer melts has been investigated.

Here, we experimentally analyse the flowing behaviour of polymer melts in diverse surface conditions of nanochannel for the first time. We functionalized the nanochannel through layer-by-layer absorption of gold nanoparticles (AuNPs) with different diameters (5 nm, 15 nm and 25 nm). Through functionalization of nanochannel, the surface properties have been manipulated. The functionalized nanochannel significantly influences the flowing behaviour of the polymer. The presence of 5 nm AuNPs monolayer enhanced the polymer flow in the nanochannel due to the increment of surface energy. However, the presence of 15 nm and 25 nm AuNPs monolayer, significantly slow down the flow of polymer melts due to the overall decrement of nanochannel diameter and increased channel roughness. The flowing behaviour of polymer melts were further enhanced under ultrasonic vibration. Due to frictional heat between the polymer melts and AuNPs, the 5 nm AuNPs monolayer enhance the flowing of polymer melts. On the other hand, the trapping of polymer chains in the valleys between 15 nm and 25 nm AuNPs, the polymer flowing behaviour is significantly affected when they flow through larger particle size AuNPs.

Experimental

Raw materials:

The following raw materials were purchased from Aldrich without further purification: auric acid ($\text{HAuCl}_4 \cdot 3\text{H}_2\text{O}$), trisodium citrate (Na_3Ct), (3-aminopropyl)-trimethoxysilane, sodium borohydride, poly styrene (PS, $M_n = 100600$, $M_w/M_n = 1.24$, Germany) and other solvents. AAO templates with 200 nm nanochannels were obtained from GE Whatman.

Synthesis of Gold nanoparticles

The different diameters AuNPs solutions were prepared following literature procedure²⁹ with modification. All glassware were rinsed in an aqua regia solution ($\text{HNO}_3/\text{HCl}=1:3$) and DI water prior to use. For 5 nm AuNPs, a 20 mL aqueous solution containing 0.75 mM $\text{HAuCl}_4 \cdot 3\text{H}_2\text{O}$ and 0.75 mM Na_3Ct was prepared at room temperature. After the addition of 0.6 mL of a 0.3 M NaBH_4 solution into the as-prepared solution under vigorous stirring, 5 nm AuNPs were formed in 10 s. For 15 nm and 25 nm AuNPs, aqueous 0.75 mM $\text{HAuCl}_4 \cdot 3\text{H}_2\text{O}$ solution was heated to 100 °C under vigorous stirring. Na_3Ct solution of 2.55 mM and 3 mM were added into $\text{HAuCl}_4 \cdot 3\text{H}_2\text{O}$ solution to get 15 nm and 25 nm AuNPs respectively. After boiling 30 minutes, the colour of the solutions changed into a wine red colour. The TEM images of AuNPs are shown in **Figure S1a-c** (Supporting Information).

Surface-modification of nanochannel

The surface-modification of nanochannel was carried out via literature procedure³⁰. At first, cleaned AAO templates were immersed into APTMS solution (2 ml APTMS, 1.5 ml DI water and 100 ml isopropanol). After keeping 1 hour at boiling temperature, APTMS modified AAO templates were rinsed with isopropanol and dried in nitrogen. After curing about 2 hours at 110 °C, the surface-modified AAO templates were used immediately. To functionalize the surface of nanochannels of AAO, about 10~15 ml of colloidal AuNPs solution was passed through the APTMS-modified AAO.

Preparation of Polymer nanowire

Polymer nanowires were prepared via literature procedures³¹. As-prepared AAO templates were assembled with polymer film and heated to a selected temperature. After several minutes, the samples were cooled to room temperature and released from the template with 1 M NaOH solution. After rinsing several times with absolute ethanol and DI water, the samples were stored in a vacuum oven to remove the solvent. The samples are denoted as PS-AAO, PS-smAAO, PS-5nm-Au, PS-15nm-Au and PS-25nm-Au which represent PS nanowire from pristine AAO, APTMS surface-modified AAO, AAO with 5 nm, 15 nm and 25 nm size AuNPs monolayer on the surface modified nanochannel respectively.

Characterization

Scanning Electron Microscopy (SEM, Philips FEG SEM XL30) was utilized to characterize the as-prepared nanowires. The surface morphologies of nanochannels of AAO were measured in air using an Atomic Force Microscope (AFM, *VEECO Multimode V*) operating at the tapping mode.

Results and discussion

Formation of AuNPs monolayer on the wall of template

The preparation procedure of AuNPs monolayer on the surface of nanochannel of AAO is presented in **Figure 1a**. At first, the inner surface of template was surface functionalized with amine groups possessing positive charge using APTMS. Under electrostatic absorption and Coulombic interaction³²⁻³⁴ between the negatively charged citrate-protected AuNPs and the amine group, the AuNPs are immobilized to form an AuNPs monolayer on the surface of the nanochannel. AuNPs colloidal solution (10~15 ml) passed through the template and formed a monolayer of AuNPs at the inner wall of the nanochannel as shown in **Figure 1b**. By controlling the diameter (5nm, 15nm, 25nm) of AuNPs, monolayers with various sizes of AuNPs (5nm, 15nm, 25nm) were formed at the inner nanochannel surface as shown in **Figure 2** and **S1e-f**. The surface roughness of the nanochannels was significantly affected by the adsorption of AuNPs. In comparison with bulk AAO, the surface roughness increased with larger size of adsorbed AuNPs.

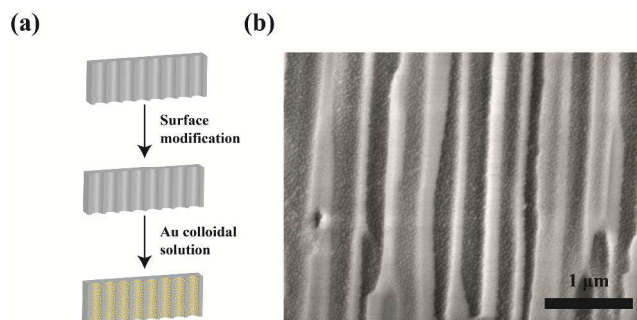


Fig. 1 (a) Schematic representation of preparation process of AuNPs monolayer in the inner nanochannel of template. (b) FESEM image of cross-section of AuNPs monolayer after passing 10~15ml 15 nm AuNPs colloidal solutions

Effect of different particle size of AuNPs monolayer on the polymer flowing behaviour

The influence of nanoparticle size on the nanoflowing behaviour of PS melts were investigated by forming monolayers of AuNPs with 5, 15 and 25 nm in the nanochannel as per previous description (**Figure 2**).

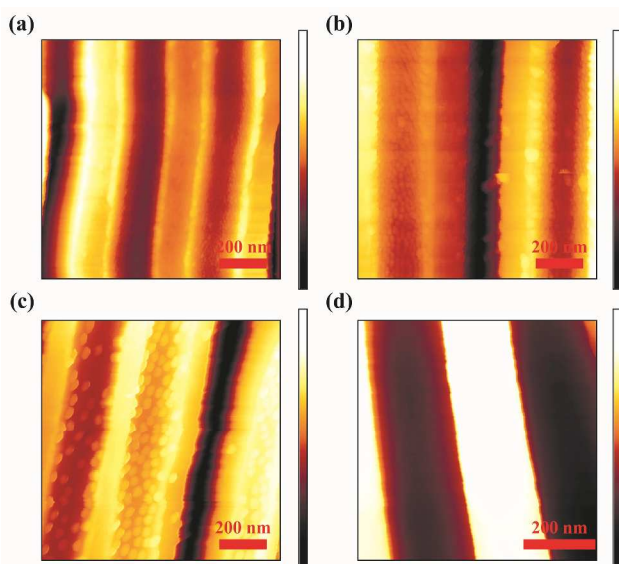


Fig. 2 AFM image of different AuNPs monolayer in the nanochannels of AAO: (a) 5 nm AuNPs monolayer; (b) 15 nm AuNPs monolayer; (c) 25 nm AuNPs monolayer; (d) bulk AAO.

The cross-sectional SEM images of PS nanowires are depicted in **Figure 3a-d**, in which the wetting temperature and wetting time were fixed at 190 °C and 10 min. The cross-sectional SEM images of PS nanowire, after wetting the nanochannel with 5, 15 and 25 nm AuNPs monolayer are depicted in **Figure 3a-c**. The cross-sectional image of PS nanowires obtained through APTMS surface-modified nanochannel is shown in **Figure 3d**. The influence of AuNPs size on the nanoflowing behaviour of polymer is shown in **Figure 3e** and **3f**. The relationship between the displacement length of PS melts with the wetting temperature at a wetting time of 10 min is depicted in **Figure 3e**. **Figure 3f** indicates the influence of wetting time on the displacement length of PS melts at a wetting temperature of 190 °C. As shown in **Figure 3a-c**, the displacement length of PS melts through AuNPs monolayer modified nanochannels are significantly influenced in comparison with those PS melts through pristine AAO. The displacement length of PS-5nm-Au (20.8 μm) exhibited obvious enhancement than that of PS-AAO (15.4 μm) as shown in **Figure S2**. However, the displacement lengths of PS-15nm-Au and PS-25nm-Au were found to be 13.3 μm and 10.8 μm respectively, shorter than the displacement length of PS-AAO. The displacement length (15.1 μm) of PS-smAAO is found to be similar as PS-AAO (15.4 μm).

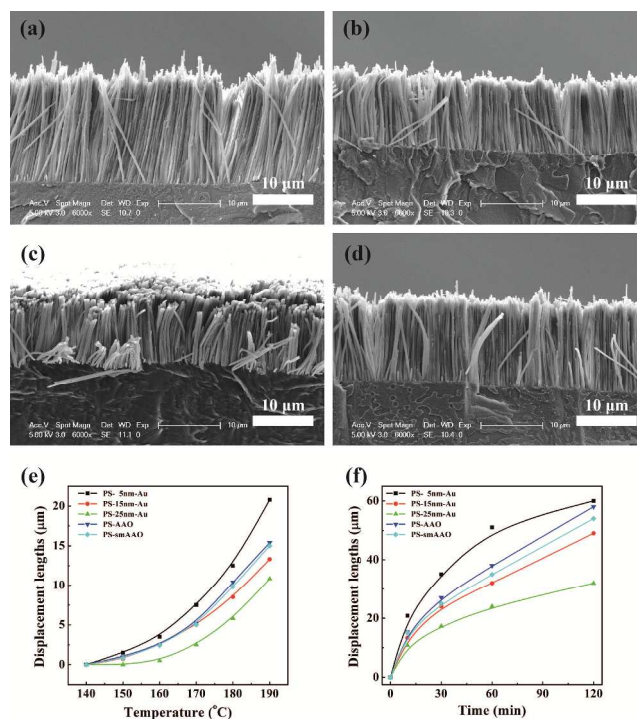


Fig. 3 SEM cross-section images of PS nanowires from different AAO template: (a), (b), (c) and (d) templates with 5 nm, 15 nm, 25 nm AuNPs monolayer and APTMS surface-modification; relationship between displacement lengths of PS nanowire and wetting temperature (e) at wetting time 10 min and wetting time (f) at wetting temperature 190 °C.

As shown in **Figure 3e** and **3f**, the wetting displacement lengths for all the samples increased with increasing wetting temperature and wetting time which is consistent with previous reports^{14, 24, 31}. For PS-5nm-Au, a significant enhancement of displacement length was found at various temperatures in comparison with other samples as shown in **Figure 3e** at a wetting time of 10 min. The displacement length of PS-25nm-Au was found to be significantly smaller than others for a wide temperature range. From 140 °C to 160 °C, the difference over the displacement length of PS-15nm-Au and PS-AAO, PS-smAAO was not found to be significant. At elevated temperature the difference over displacement length became obvious. At a wetting temperature of 190 °C, the displacement length of PS-AAO and PS-smAAO became 15.4 μm and 15 μm respectively, higher than PS-15nm-Au (13.3 μm). A longer wetting time also increases the displacement length of all the samples as shown in **Figure 3f** at a wetting temperature of 190 °C. The displacement length of PS-5nm-Au sharply increased and achieved around 60 μm (thickness of AAO) at a wetting time of 120 min. In comparison with PS-AAO, PS-smAAO and PS-15nm-Au, a similar trend with shorter displacement length was observed. The displacement length of PS-25nm-Au was significantly shorter than other samples. At a wetting time of 120 min, the displacement length of PS-25nm-Au was found to be 32.1 μm.

As mentioned, the ultrasonic vibration is found to enhance the nanoflow of polymer melts in the nanochannels. The nanoparticle/polymer composite exhibited a substantial

increment of displacement length than pure polymer melts under ultrasonic vibration. However, the mechanism of enhancement is unclear. To investigate the interaction between the polymer chain and the nanoparticle under ultrasonic vibration, various ultrasonic vibration frequencies were applied to enhance the nanoflow of PS melts at a wetting temperature of 190 °C and wetting time of 10 min, as shown in **Figure 4**. The displacement lengths of PS-5nm-Au, PS-15nm-Au and PS-25nm-Au under 60 kHz ultrasonic vibrations are shown in **Figure 4a-c**. **Figure 4d** represents the relationship between the displacement length and ultrasonic vibration from 10 kHz to 60 kHz. In comparison, with static condition, the displacement lengths of PS-5nm-Au, PS-15nm-Au and PS-25nm-Au under 60 kHz ultrasonic vibration increased from 20.8 μm, 13.3 μm and 10.8 μm to 54.0 μm, 23.4 μm and 19.52 μm, respectively. The displacement lengths of PS-AAO and PS-smAAO were also enhanced under ultrasonic vibration. In comparison with PS-15nm-Au and PS-25nm-Au, a sharp increment for PS-5nm-Au was observed. The displacement length of PS-25nm-Au has no significant changes from 10 kHz to 30 kHz in comparison with other samples.

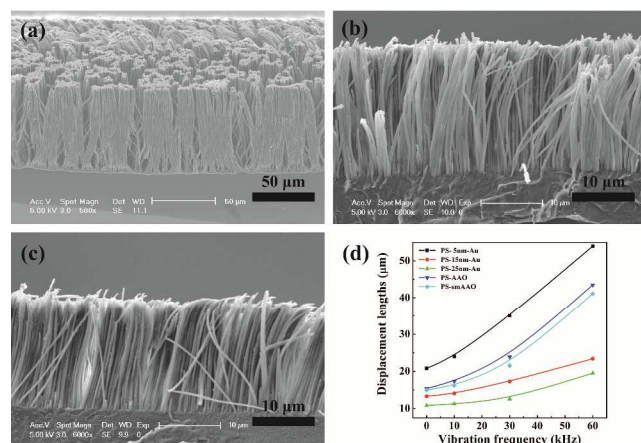


Fig. 4 SEM cross-section images of PS-5nm-Au (a), PS-15nm-Au (b) and PS-25nm-Au (c) under 60 kHz ultrasonic vibration at wetting temperature 190 °C and wetting time of 10 min, (d) relationship between displacement length of samples and vibration frequency.

The flowing behaviour of polymer melts in nanoconfinement such as 1-D nanochannel are influenced by many factors such as viscosity of polymer melts, molecular weight of polymer, temperature, time and surface energy of template. As discussed above, for all samples, the wetting temperature and time significantly influence the nanoflow of polymer melts and consistent with the results of **Figure 3e** and **3f**. Higher wetting temperature enhances nanoflow by decreasing the viscosity of polymer melts. Elongation of wetting time lead to long displacement of polymer melts. Conventional theory such as Hagen-Poiseuille equation about nanofluidics in nanopipes/nanochannels is based on the assumption that the liquid in the nanopipes/nanochannels is Newtonian flow which is incompressible fluid. Even for simple liquids such as water, ethanol, and decane, the conventional theory could not explain

the experimental results. Hence, for the complex system such as polymer melts with different molecular weights, the conditions become even more complex. The above results might be qualitatively explained by Washburn equation as follows:

$$L(t)^2 = (R\gamma\cos\theta/2\eta)t \quad (1)$$

with $L(t)$ being the displacement length of polymer melts in nanochannels, R the radius of nanochannel, η the shear viscosity of polymer melts, γ the polymer melts/vapor surface tension and t wetting time of polymer melts in nanochannel. Through surface-modification of nanochannel with a surfactant, the surface energy of nanochannel is modified. The PS-smAAO exhibits slight reduction in displacement length in comparison with PS-AAO due to the decreased surface energy. The polymer melts/vapor surface tension, γ , is the driving force of nanoflow of polymer melts. The ATPMS on the inner surface of nanochannel reduce the surface energy and further decrease the driving force which directly leads to the reduction of displacement length of polymer melts. In comparison with the aliphatic ending group of surfactant such as octadecyltrimethoxysilane¹⁴, the decrease in the displacement length is less obvious. The appearance of AuNPs monolayer in nanochannels not only changes the surface energy, but also significantly affects the surface roughness and the diameter of nanochannel. For PS-5nm-Au, the surface roughness and diameter of nanochannels are not significantly affected as PS-15nm-Au and PS-25nm-Au. Although with the reduction of 5 nm in diameter of nanochannel and increase of surface roughness, the surface energy was still increased for 5 nm AuNPs. Comparing PS-5nm-Au, PS-15nm-Au and PS-25nm-Au, an increase in the diameter of AuNPs size significantly affected the diameter and roughness of nanochannel. Although the surface energy of nanochannel is increased due to the presence of AuNPs, the decrease in the diameter of nanochannel and the increased surface roughness lead to smaller displacement length of polymer melts as shown **Figure 3e** and **3f**. For the flowing behaviour of polymer melts in a nanoscale channel, not only the bulk properties such as η and γ , but also the interaction of polymer melts with nanochannel wall affects the flowing behaviour. From **Figure 3e** and **3f**, as the diameter of AuNPs increased from 5 nm to 15 nm and 25 nm, the displacement length of PS sharply reduced at all wetting temperatures. The onset of wetting temperature for PS-25nm-AAO is shifted about 10 °C from 140 °C to 150 °C. For PS-5nm-Au, an increase in the surface energy plays a critical role on the enhancement of nanoflow. For 15 nm and 25 nm AuNPs monolayers, the polymer flowing behaviour in nanochannels is affected by two aspects: first, the roughness of nanochannel is increased due to larger diameter of AuNPs. With increased roughness, the binding effect between the wall and polymer chain plays a crucial role. Due to stronger binding effect, the polymer chains are trapped into the valleys between AuNPs. Moreover, simulation results showed that the increase in surface roughness drastically reduces the slippage of simple liquid and polymer melts³⁵⁻³⁷. Secondly, the diameter of

nanochannel is modified by the presence of AuNPs. The average diameter of nanochannel is around 200 nm. The presence of 15 nm and 25 nm AuNPs in the channel decreases the average diameter, 200 nm, of nanochannels to 170 nm and 150 nm respectively. According to the Washburn equation, the $L(t)$ have relationship with R , the radius of nanochannel. Due to above reasons, the displacement lengths of PS-15nm-Au and PS-25nm-Au were decreased.

Enhanced polymer flowing behaviour due to ultrasonic vibration has been investigated. The displacement length of PS melts in nanochannel is enhanced for the frequency from 10 kHz to 60 kHz in comparison with static condition. The enhanced flowing behaviour may be attributed to several reasons. The first reason is the reduction of viscosity of PS melts. According to the Arrhenius equation:

$$\ln(\eta) = \ln(A) + \Delta E_{\eta}/RT \quad (2)$$

Where A is the constant relative to the polymer molecular structures, ΔE_{η} is the flowing active energy of polymer melts. R and T are gas constant and melts temperature respectively. Due to short relaxation time of ultrasonic vibration, the entanglements of polymer chains are promoted and further lead to activate the wriggling motion of polymer chain and reduce the polymer melts elasticity and interaction among polymer chain. As a result, the ΔE_{η} is decreased and reduces the viscosity of polymer melts. Finally, the $L(t)$ is enhanced according to the Washburn equation. Another reason would be the surface friction between polymer chain and nanochannel wall. Under ultrasonic vibration, the friction occurs between the polymer chain and wall. Here, the mechanical energy is converted into heat energy and increasing the temperature between the polymer melts and nanochannel wall eventually decreases the viscosity of polymer melts. The presence of AuNPs increases the roughness of nanochannel wall. For PS-5nm-Au, the heat originated from the friction enhanced the flowing behaviour of polymer melts from 10 kHz to 60 kHz. However, the PS-15nm-Au and PS-25nm-Au exhibited smaller enhancement in comparison with PS-5nm-Au. Although the frictional heat decreases the viscosity of polymer melts, the polymer chains which are trapped between larger size AuNPs would be not easily released.

Conclusion

Through surface-modification of nanochannel with various size gold nanoparticles, the flowing behaviour of polymer melts under diverse surface conditions have been systematically investigated. In comparison with pristine AAO, the uniform distribution of 5 nm AuNPs monolayer on the nanochannel wall enhances the flow of polymer melts due to increase in the surface energy. A further increase in the diameter of AuNPs in the nanochannel increases the surface roughness and the flowing behaviour of polymer melts was significantly affected. Moreover, under ultrasonic vibration, 5 nm AuNPs have higher displacement length than other size AuNPs due to the generation of heat by friction between the polymer melts and

AuNPs. We anticipate that these results would provide fundamental information on the preparation of one-dimensional polymer nanochannels, micro/nano-fluidic channels and potentially could be applied for micro/nano-injection technology.

Acknowledgements

We acknowledge grants from City University of Hong Kong's Strategic Research Grant Project no. 7004012, the Research Grants Council of the Hong Kong Special Administrative Region (Project No.T23-713/11) and Shenzhen Municipality project no. JCYJ20120618115445056. Authors acknowledge Professor Jonathan Wylie of Mathematics department for fruitful discussion and Mr. Wei Chen on surface modification.

Notes and references

^a Centre of Super-Diamond and Advanced Films (COSDAF), Department of Physics and Materials Science, City University of Hong Kong, Hong Kong SAR E-mail: val.roy@cityu.edu.hk

^b Shenzhen Research Institute, City University of Hong Kong, High-Tech Zone, Nanshan District, China.

1. S. Supple and N. Quirke, *Physical Review Letters*, 2003, 90, 214501.
2. Y. Li, J. Xu and D. Li, *Microfluidics and Nanofluidics*, 2010, 9, 1011-1031.
3. C. Martin and P. Kohli, *Nature reviews. Drug discovery*, 2003, 2, 29-37.
4. A. Srivastava, O. Srivastava, S. Talapatra, R. Vajtai and P. Ajayan, *Nature Materials*, 2004, 3, 610-614.
5. M. Steinhart, *Advances in Polymer Science*, 2008, 220, 123-187.
6. J. E. Slota, X. M. He and W. T. S. Huck, *Nano Today*, 2010, 5, 231-242.
7. Y. Yang, K. Mielczarek, M. Aryal, A. Zakhidov and W. Hu, *Acs Nano*, 2012, 6, 2877-2892.
8. A. del Campo and E. Arzt, *Chemical Reviews*, 2008, 108, 911-945.
9. P. Kenis, R. Ismagilov, S. Takayama, G. Whitesides, S. Li and H. White, *Accounts Of Chemical Research*, 2000, 33, 841-847.
10. M. Whitby and N. Quirke, *Nature nanotechnology*, 2007, 2, 87-94.
11. M. K. Byong, S. Shashank and H. B. Haim, *Nano Letters*, 2004, 4.
12. C.-S. Chen, S.-C. Chen, W.-L. Liaw and R.-D. Chien, *European Polymer Journal*, 2008, 97, 2527-2532.
13. R.-D. Chien, W.-R. Jong and S.-C. Chen, *Journal Of Micromechanics And Microengineering*, 2005, 15, 1389.
14. K. Yung, L. He, Y. Xu and Y. Shen, *Polymer*, 2006, 47, 4454-4460.
15. A. Rawool, S. Mitra and S. Kandlikar, *Microfluidics and Nanofluidics*, 2006, 2, 215-221.
16. Y. Xin and T. Z. Lucy, *Microfluidics and Nanofluidics*, 2012, 14.
17. L. Joly, C. Ybert and L. Bocquet, *Physical Review Letters*, 2006, 96, 046101.
18. T. Schmatko, H. Hervet and L. Leger, *Physical Review Letters*, 2005, 94, 244501.
19. K. B. Migler, H. Hervet and L. Leger, *Physical Review Letters*, 1993, 70, 287-290.
20. C. I. Bouzigues, P. Tabeling and L. Bocquet, *Physical Review Letters*, 2008, 101, 114503.

21. P. Joseph, C. Cottin-Bizonne, J. M. Benoit, C. Ybert, C. Journet, P. Tabeling and L. Bocquet, *Physical Review Letters*, 2006, 97, 156104.
22. Y. X. Zhu and S. Granick, *Physical Review Letters*, 2002, 88, 106102.
23. T. Schmatko, H. Hervet and L. Léger, *Langmuir : the ACS journal of surfaces and colloids*, 2006, 22, 6843-6850.
24. K.-L. Yung, J. Kong and Y. Xu, *Polymer*, 2007, 48, 7645-7652.
25. J. Kong, Y. Xu, K. Yung, Y. Xie and L. He, *The Journal of Physical Chemistry C*, 2009, 113, 624-629.
26. W. Tian, K. Yung, Y. Xu, L. Huang, J. Kong and Y. Xie, *Nanoscale*, 2011, 3, 4094-4100.
27. M. Steinhart, J. H. Wendorff, A. Greiner, R. B. Wehrspohn, K. Nielsch, J. Schilling, J. Choi and U. Gosele, *Science*, 2002, 296, 1997-1997.
28. M. Steinhart, in *Self-Assembled Nanomaterials II: Nanotubes*, ed. T. Shimizu, 2008, vol. 220, pp. 123-187.
29. X. Ji, X. Song, J. Li, Y. Bai, W. Yang and X. Peng, *Journal Of The American Chemical Society*, 2007, 129, 13939-13948.
30. S. Flink, F. van Veggel and D. N. Reinhoudt, *J. Phys. Org. Chem.*, 2001, 14, 407-415.
31. W. Tian, K. L. Yung, Y. Xu, L. Huang, J. Kong and Y. Xie, *Nanoscale*, 2011, 3, 4094-4100.
32. K. C. Grabar, P. C. Smith, M. D. Musick, J. A. Davis, D. G. Walter, M. A. Jackson, A. P. Guthrie and M. J. Natan, *Journal Of The American Chemical Society*, 1996, 118, 1148-1153.
33. K. C. Grabar, R. G. Freeman, M. B. Hommer and M. J. Natan, *Analytical Chemistry*, 1995, 67, 735-743.
34. R. G. Freeman, K. C. Grabar, K. J. Allison, R. M. Bright, J. A. Davis, A. P. Guthrie, M. B. Hommer, M. A. Jackson, P. C. Smith, D. G. Walter and M. J. Natan, *Science*, 1995, 267, 1629-1632.
35. A. Niavarani and N. V. Priezjev, *J. Chem. Phys.*, 2008, 129.
36. Y. Li, J. Xu and D. Li, *Microfluidics and nanofluidics*, 2010, 9, 1011-1031.
37. P. A. Thompson and S. M. Troian, *Nature*, 1997, 389, 360-362.